

Thermally Tunable Photonic Filter for WDM Networks Using 1D Superconductor Dielectric Photonic Crystals

Maitreyi Upadhyay¹ · Suneet K. Awasthi¹ · Laxmi Shiveshwari² · Pankaj K. Srivastava³ · Sant P. Ojha⁴

Received: 3 March 2015 / Accepted: 9 March 2015 / Published online: 26 March 2015
© Springer Science+Business Media New York 2015

Abstract A novel design of a single-channel thermally tunable photonic filter by cascading two one-dimensional (1D) superconductor-dielectric photonic crystals (SDPCs) through low loss silica fiber for wavelength selective switching (WSS) application is being presented theoretically. This filter is capable to separate and switch unique wavelength channel (without interfering with each other) from 12 equally spaced wavelength channels adopted by the International Telecommunication Union (ITU). It may be used in wavelength division multiplexing (WDM)-based optical networks for routing signals at specific wavelengths into an optical fiber with minimum distortion. This idea may also be explored in the design of very precise thermal sensing devices for remote sensing applications.

Keywords Photonic crystals (PCs) · Transfer matrix method (TMM) · Optical filters · Wavelength division multiplexing (WDM) · Superconductor

✉ Suneet K. Awasthi
suneet_electronic@yahoo.com

¹ Department of Physics and Material Science and Engineering, Jaypee Institute of Information Technology, Noida 201304, India

² Department of Physics, K B Women's College (A Constituent Unit of Vinoba Bhave University), Hazaribag 825301, India

³ Department of Mathematics, Jaypee Institute of Information Technology, Noida 201304, India

⁴ Department of Applied Physics, Institute of Technology, Banaras Hindu University, Varanasi 221005, India

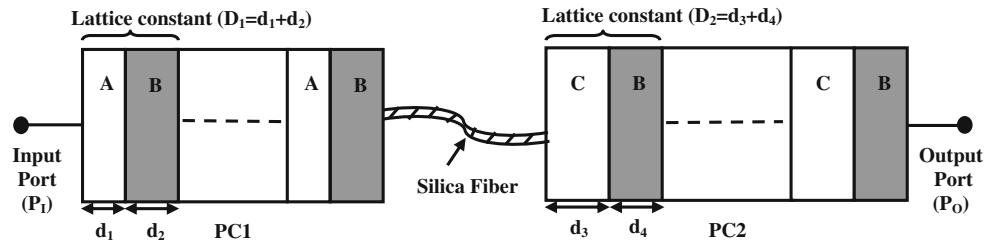
1 Introduction

Optical filters capable of switching and routing optical signals, at a particular wavelength channel, carrying optical data from multichannel wavelength network into an optical fiber with minimum distortions are the key elements in modern computation and communication systems because optical signal can handle large bandwidth and large information flow with very high speed [1, 2].

During the past two and half decades, optical filters based on one-dimensional photonic crystals (1D PCs) have inspired a lot of attention and investigation due to their important applications in modern photonic engineering including optical communication and optoelectronics. PCs are structures with periodically modulated dielectric constants whose distribution follows periodicity of the order of a fraction of the optical wavelength [3]. On account of the wave nature of light and interference caused by the periodic structure, photonic bandgaps (PBGs) are created. Photons with energies lying in the bandgap cannot propagate through the structure, while those with energies lying outside the bandgap can do so [4]. Thus, they have very useful optical properties of technical interest [5], for instance, narrow and high band pass filters, omnidirectional mirrors, tunable optical switches, multi-channel, and single-channel optical filters etc. [6–9]. This active research area has been extended to superconductor-dielectric photonic crystals (SDPCs), due to their special features over conventional all dielectric and metal dielectric PCs [10–13]. One such feature is to tune their PBGs externally by changing the temperature of superconductor without disturbing the experimental arrangement [13, 14].

In the present communication, we have proposed a single-channel thermally tunable photonic filter (TTPF) for

Fig. 1 A schematic design of TTPF system by cascading two 1D SDPC (PC₁ and PC₂) side by side through low loss silica fiber



wavelength-selective switching (WSS) applications by cascading two 1D SDPCs (PC₁ and PC₂) side by side through low loss silica fiber. The transmission properties of 1D SDPC-based TTPF are investigated through transfer matrix method (TMM) [8, 15]. For proper working of the proposed filter, very precise control of temperatures of PC₁ and PC₂ is required. Therefore high-precision temperature control and stabilization technique [16] using cryocooler can be used to achieve the same.

The structure of the paper is organized as follows: The model and corresponding analytical formulae, such as effective refractive index of the superconductor (SC) and transmission coefficients are introduced in Section 2. Numerical results are presented and discussed in Section 3. Finally, conclusions are given in Section 4.

2 Theoretical Formulation

Block diagram of the proposed TTPF for WSS-based optical networks by cascading two 1D SDPC (PC₁ and PC₂) through low loss silica fiber is shown in Fig. 1. Here, PC₁ and PC₂ are put close to each other in such a way that radiation after passing through PC₁ is allowed to fall normally on PC₂ through low loss silica fiber. The lattice constants of PC₁ and PC₂ are denoted by $D_1 = d_1 + d_2$ and $D_2 = d_3 + d_4$, respectively. Here, d_1, d_2 and d_3, d_4 denote the thicknesses of low temperature SC (niobium [Nb]), dielectric (barium fluoride [BaF₂]) of PC₁ and high temperature SC (yttrium barium copper oxide [YBa₂Cu₃O₇]), dielectric (barium fluoride (BaF₂)) of PC₂. The entire TTPF is assumed to be surrounded by air with a refractive index 1. TMM is used to calculate the transmittance of PC₁ and PC₂ at normal incidence [8, 15]. The characteristic matrix $M(\Lambda)$ of one period is given by [15]

$$M(\Lambda) = \prod_{j=1}^2 \begin{pmatrix} \cos \delta_j & -\frac{i}{q_j} \sin \delta_j \\ -iq_j \sin \delta_j & \cos \delta_j \end{pmatrix} \quad (1)$$

$$= \begin{bmatrix} M_{11} & M_{12} \\ M_{21} & M_{22} \end{bmatrix},$$

where $\delta_j = \frac{2\pi}{\lambda_0} n_j d_j$, with $q_j = n_j$, ($j = \text{SC}, D$), and λ_0 is the free space wavelength. Here, n_j and d_j denote the refractive index and thickness of the j th layer respectively.

For a N period structure, the characteristic matrix of the medium is given by

$$[M(\Lambda)]^N = M_{SC} M_D M_{SC} M_D \dots M_{SC} M_D \quad (2)$$

$$= \begin{pmatrix} m_{11} & m_{12} \\ m_{21} & m_{22} \end{pmatrix}.$$

where m_{11}, m_{12}, m_{21} , and m_{22} are the matrix elements of $[M(\Lambda)]^N$ which represents the total transfer matrix.

The transmission coefficient t of the multilayer periodic structure is given by

$$t = \frac{2 q_1}{(m_{11} + m_{12} q_k) q_1 + (m_{21} + m_{22} q_k)} \quad (3)$$

where q_1 and q_k represent the coefficients of medium on either side of the structure. Since the entire structure is surrounded by air, $q_1 = q_k = n_o$. Here, n_o is the refractive index of air with value 1. The transmittance of the multilayer [15] is given by

$$T = |t|^2 \quad (4)$$

In order to describe electromagnetic response of both superconductors, Gorter-Casimir two fluid model [11, 17] in the absence of external magnetic field is adopted. The frequency and temperature-dependent effective relative permittivity of a superconductor is given by [17]

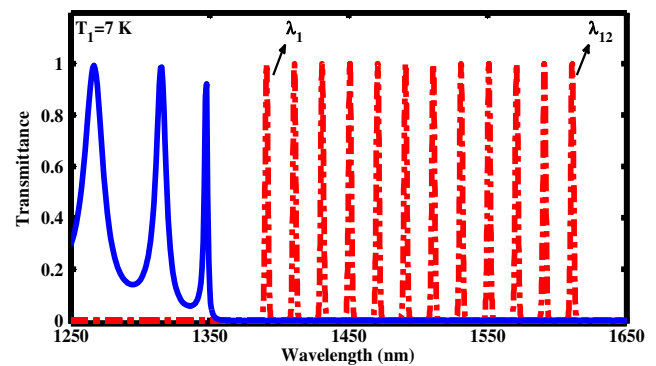


Fig. 2 Transmittance spectra (blue color) of PC₁ ($d_1 = 40$ nm, $d_2 = 248$ nm, $N = 12$, and $T_1 = 7.0$ K) at normal incidence. Also shown are 12 discrete wavelength channels (red color) injected from input port P₁ into PC₁. These channels with separation 20 nm and width 1 nm fall within the PBG of PC₁

Table 1 List of 12 WDM channels with specific wavelength, separation, and line width of input signal

Wavelength channels	Specific wavelength (nm)	Separation (nm)	Line width (nm)
λ_1	1391	20	1
λ_2	1411	20	1
λ_3	1431	20	1
λ_4	1451	20	1
λ_5	1471	20	1
λ_6	1491	20	1
λ_7	1511	20	1
λ_8	1531	20	1
λ_9	1551	20	1
λ_{10}	1571	20	1
λ_{11}	1591	20	1
λ_{12}	1611	20	1

$$\varepsilon_i(\omega, T) = \varepsilon_c - \frac{c^2}{\omega^2[\lambda_L(0)]^2} \left[1 - \left(\frac{T}{T_c} \right)^p \right] - \frac{c^2}{\omega(\omega+i\gamma)[\lambda_L(0)]^2} \left(\frac{T}{T_c} \right)^p \tag{5}$$

where ε_c is the dielectric constant of the crystal, and ω and c are the frequency and speed of electromagnetic wave in vacuum, respectively. $\lambda_L(0)$ is the London penetration depth at temperature $T = 0$ K, and T_c is the transition temperature of the superconductor. The value of exponent p is 2 and 4 to represent high and low temperature SC, respectively. Here, γ represents damping term due to normal conducting electrons. The third term on the right-hand side of (5) is omitted by neglecting the contribution of normal conducting electrons because the results obtained by

two methods—neglecting and not neglecting this contribution are almost the same as described in [10]. Thereby, the temperature-dependent effective refractive index of lossless superconductor takes the form

$$n_i = \sqrt{\varepsilon_i(\omega, T)} = \sqrt{\varepsilon_c - \frac{c^2}{\omega^2[\lambda_L(0)]^2} \left[1 - \left(\frac{T}{T_c} \right)^4 \right]} \tag{6}$$

3 Results and Discussion

In the following numerical calculations, we have taken $(AB)^N$ as 1D SDPC (PC₁) composed of two alternating layers of low temperature SC (A) and conventional material (B). The conventional material is taken as dielectric BaF₂ with relative permittivity (ε_B) 2.13 and low temperature SC is niobium (Nb). The transition temperature (T_c^A) and London penetration depth at zero temperature ($\lambda_L(0)$) of Nb are 9.2 K and 40 nm, respectively, as reported in [6]. Though in the region of present investigation, superconductors may be lossy even below the transition temperature, but for simplicity, the losses in superconductors Nb and YBa₂Cu₃O₇ both are neglected. For the proposed 12-period structure PC₁, we have chosen the thicknesses of layers A (B) as 40 (248) nm in order to get a PBG in the near-infrared spectral region (1250 to 1650 nm) at a temperature of 7.0 K because it is a low-loss region in silica fibers [18].

We have first calculated (using TMM) the transmission spectra at normal incidence to get a PBG in PC₁ in the region of investigation. Then, transmittance is plotted as a function of wavelength (Fig. 2). It is observed that a PBG occurs in the near-infrared region which extends from $\lambda_l = 1366$ nm to $\lambda_r = 1650$ nm which lies within

Table 2 Control table of TTPFS for selecting different wavelength channels

S. no.	T_1 (K)	PC ₁		PC ₂		
		PBG (nm)	Selected wavelength at silica fiber	T_2 (K)	PBG (nm)	Selected wavelength at P_o
1	7.28	1403–1650	λ_1	41.0	1250–1385	λ_1
2	7.39	1421–1650	$\lambda_1 + \lambda_2$	57.5	1250–1404	λ_2
3	7.48	1444–1650	λ_1 to λ_3	65.7	1250–1422	λ_3
4	7.57	1463–1650	λ_1 to λ_4	71.2	1250–1440	λ_4
5	7.65	1484–1650	λ_1 to λ_5	75.3	1250–1457	λ_5
6	7.72	1505–1650	λ_1 to λ_6	78.6	1250–1479	λ_6
7	7.79	1525–1650	λ_1 to λ_7	81.3	1250–1498	λ_7
8	7.85	1545–1650	λ_1 to λ_8	83.6	1250–1515	λ_8
9	7.91	1566–1650	λ_1 to λ_9	85.6	1250–1540	λ_9
10	7.96	1585–1650	λ_1 to λ_{10}	87.2	1250–1557	λ_{10}
11	8.00	1604–1650	λ_1 to λ_{11}	88.7	1250–1576	λ_{11}
12	8.05	1633–1650	λ_1 to λ_{12}	90.0	1250–1595	λ_{12}

the spectral band (1260–1675 nm) used for optical fiber communications.

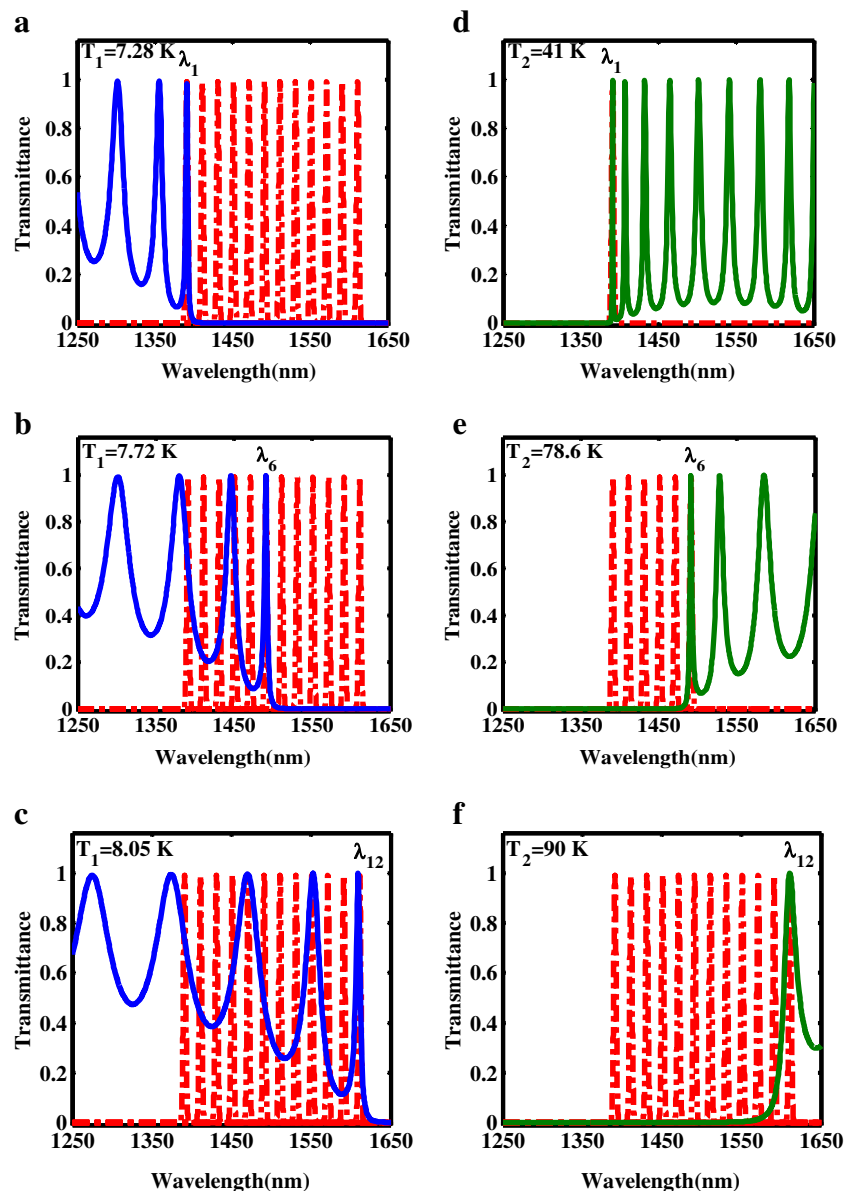
We present the working principle of the proposed TTPF composed of two 1D SDPCs (PC_1 and PC_2) for WSS-based optical networks. Consider an input signal consisting of 12 independently modulated light sources emitting signals each of at a unique wavelength ranging from 1391 to 1611 nm (listed in Table 1) is incident normally on PC_1 through input port P_I (Fig. 1). Since all these wavelengths lie within the PBG of PC_1 (Fig. 2), they will be reflected by PC_1 and will not reach low loss silica fiber as shown in Fig. 1.

Next, we have chosen another 1D SDPC (PC_2) composed of two alternating layers of high-temperature SC (C) and conventional material (B). The conventional material is again taken as dielectric BaF_2 with relative permittivity

(ϵ_B) 2.13 and thickness 248 nm as that of PC_1 . The high-temperature SC is taken as $YBa_2Cu_3O_7$ with $\lambda_L(0) = 145$ nm and $T_C^C = 93$ K as reported in [19]. The total number of periods of PC_2 is also 12. Here, thickness and temperature of the layer C is selected as 350 nm and 41 K, respectively, in order to get a narrower PBG extending from 1250 to 1385 nm in the near-infrared region.

Further, PC_1 and PC_2 are put close to each other in such a way that radiation after passing through PC_1 falls normally at PC_2 through low loss silica fiber (Fig. 1). Since the refractive index of SC layer is dependent on London penetration depth and external temperature both, therefore, by changing the temperature of the SC layer, its refractive index can be changed and hence the extent of the PBG. As we increase the temperature (T_1) of PC_1 from 7.28

Fig. 3 Working principle of TTPFS for wavelength selective switching application. **a–c** Transmittance spectra at normal incidence (blue color) for PC_1 ($d_1 = 40$ nm, $d_2 = 248$ nm, and $N = 12$) at $T_1 = 7.28$ K, 7.72 K, and 8.05 K. Also shown are 12 discrete wavelength channels (red color) injected from input port P_I into PC_1 . **d–f** Transmittance spectra (green color) for PC_2 ($d_3 = 350$ nm, $d_4 = 248$ nm, and $N = 12$). The discrete wavelength channels transmitted by PC_1 and incident normally on PC_2 via low loss silica fiber are shown in red color. PC_2 transmits the wavelength channels λ_1 , λ_6 , and λ_{12} at $T_2 = 41$ K, 78.6 K, and 90 K, respectively



to 8.05 K below T_c^A , PBG of PC₁ starts to shrink in the region of investigation and shift towards the higher side of the wavelength, thus allowing different unique wavelength channels of input signal to pass through PC₁ via low loss silica fiber and reach normally at PC₂ (Table 2). In order to switch desired wavelength channels from PC₂, we vary the temperature of PC₂ from 41 to 90 K ($T_2 < T_c^C$), which causes the PBG of PC₂ to expand and move towards the higher side of the wavelength. This temperature-dependent PBG reflects all the wavelength channels of input radiation coming out from PC₁ and transmits only one wavelength channel depending upon the temperature of PC₂ to reach at output port (P_o) as shown in Fig. 3. Table 2 shows how PC₁ and PC₂ can be cascaded side by side through low loss silica fiber to separate and switch-specific wavelength channels without interfering with each other amongst equally spaced 12 wavelength channels each having full width at half maximum (FWHM) of 1 nm as per the WDM standards developed by the International Telecommunication Union (ITU) specifying channel spacing in terms of frequency (wavelength) for wavelength selective switching applications [18].

The WSS behavior of the proposed photonic filter does not affect the intensity and FWHM of individual WDM channels; it thus eliminates the drawbacks for switching applications associated with 1D defect photonic crystals (DPCs) [14–17]. Moreover, for achieving wavelength selective switching from 1D DPCs to switch large number of closely spaced wavelength channels, crosstalk between adjacent channels should also be taken into account. For better performance of the filter, its value must be small enough. Contrary to this, in the proposed design, crosstalk does not have any significant contribution over the filter performance due to the synchronize tuning between the PBGs of PC₁ and PC₂ to allow only one wavelength channel to reach at P_o .

4 Conclusions

A new and simple design of single-channel TTPF composed of two 1D SDPCs (PC₁ and PC₂) connected through low loss silica fiber, which is capable of separating and switching unique wavelength channels without interfering with each other amongst 12 equally spaced wavelength channels, is presented. Each channel has FWHM of 1 nm as per the WDM standards developed by the ITU specifying channel spacing in terms of frequency (wavelength). The proposed TTPF that performs channel selection for WSS applications may play an important role for designing some new kind of optical cross-connect switches to achieve high degree of path-configuration modularity, capacity of scaling, and flexibility in adding dropping channels at a client site. This idea

may also be used to achieve high-precision thermal sensing in remote sensing applications.

Acknowledgments The authors would like to thank Retd. Prof. and Head Department of Physics Dr. U. Malaviya of University of Lucknow for the useful discussions and her support during work. One of the authors Dr. Suneet Kumar Awasthi wishes to thank his wife Mrs. Shraddha Awasthi and his son master Bhavya Awasthi for their support during the preparation of this manuscript.

Conflict of interest Authors do not have any conflict of interest pertaining to this work.

References

1. Kabilan, A.P., Christina, X.S., Caroline, P.E.: International conference on optics and photonics. http://www.csio.res.in:8080/icop/contents/Poster/Poster%20Session%203/Photonic%20Bandgap%20Material/PS3_C.1_A.P.%20Kabilan%201.pdf (2009)
2. Gance, B.: Wavelength tunable add/drop optical filter. *IEEE Photon. Technol. Lett.* **8**, 245–247 (1996)
3. Wu, J.J., Gao, J.X.: Transmission properties of Fibonacci quasi-periodic one-dimensional superconducting photonic crystals. *Optik* **123**, 986–988 (2012)
4. Jaonnopoulos, J.D., Villeneuve, P.R., Fan, S.: Photonic crystals: putting a new twist on light. *Nature* **386**, 143–149 (1997)
5. Mishra, A., Awasthi, S.K., Srivastava, S.K., Malaviya, U., Ojha, S.P.: Tunable and omnidirectional filters based on one dimensional photonic crystals composed of single negative materials. *JOSA B* **28**, 1416–1422 (2011)
6. Dai, X.Y., Xiang, Y.J., Wen, S.C.: Broad omnidirectional reflector in the one dimensional ternary photonic crystals containing superconductor. *PIER* **120**, 17–34 (2011)
7. Wang, Z., Guo, C., Jiang, W.: Omnidirectional reflection extension in a one dimensional superconducting dielectric binary graded photonic crystals with graded geometric layers thicknesses. *PIER Lett.* **42**, 13–22 (2013)
8. Awasthi, S.K., Malaviya, U., Ojha, S.P.: Enhancement of omnidirectional total-reflection wavelength range by using one-dimensional ternary photonic bandgap material. *JOSA B* **23**, 2566–2571 (2006)
9. Upadhyay, M., Awasthi, S.K., Srivastava, S.K., Ojha, S.P.: Infrared omnidirectional mirror based on one-dimensional birefringent-dielectric photonic crystal. *PIER M* **25**, 211–222 (2012)
10. Li, C.Z., Liu, S.B., Kong, X.K., Bain, B.R., Zhang, X.Y.: Tunable photonic bandgap in a one dimensional superconducting dielectric superlattice. *Appl. Opt.* **50**, 2370–2375 (2011)
11. Wu, C.J., Liu, C.L., Yang, T.J.: Investigation photonic band structure in a one-dimensional superconducting photonic crystal. *JOSA B* **26**, 2089–2094 (2009)
12. Hsu, H.T., Kuo, F.Y., Wu, C.J.: Optical properties of a high-temperature superconductor operating in near zero-permittivity region. *J. Appl. Phys.* **107**, 053912 (2010)
13. Upadhyay, M., Awasthi, S.K., Shiveshwari, L., Shukla, S.N., Ojha, S.P.: Two channel thermally tunable band stop filter for wavelength selective switching applications by using 1D ternary superconductor photonic crystal. *J. Supercond. Nov. Magn.* (2015). doi:10.1007/s10948-015-2969-x
14. Srivastava, S.K.: Study of defect modes in 1d photonic crystal structure containing high and low T_c superconductor as a defect layer. *J. Supercond. Nov. Magn.* **27**, 101–114 (2014)

15. Born, M., Wolf, E.: Basic properties of the electromagnetic field. In Principles of optics, pp. 1–70. Cambridge U Press (1980)
16. Hasegawa, Y., Nakamura, D., Murata, M., Yamamoto, H., Komine, T.: High precision temperature control and stabilization using a cryocooler. *Rev. Sci. Instrum.* **81**, 094901 (2010)
17. Chang, T.W., Liu, J.W., Yang, T.J., Wu, C.J.: Analysis of transmission properties in a photonic quantum well containing superconducting materials. *PIER* **140**, 327–340 (2013)
18. Keiser, G.: Overview of optical fiber communications. In: Optical Fiber Communications. 4th edn. (2012)
19. Marouchkine, A. Room temperature superconductivity, 1st edn. Cambridge International Science Publishing, U. K. (2004)